Available online at www.sciencedirect.com
ScienceDirect
Journal of Pharmaceutical and Biomedical Analysis 45 (2007) 201–210
JOURNAL OF PHARMACEUTICAL AND BIOMEDICAL ANALYSIS
www.elsevier.com/locate/jpba

Structural identification and characterization of potential impurities of pantoprazole sodium[1]

Ganta Madhusudhan Reddy[a,c], B. Vijaya Bhaskar[a], P. Pratap Reddy[a], S. Ashok[a], P. Sudhakar[b], J. Moses Babu[b,*], K. Vyas[b], K. Mukkanti[c]

[a] *Research & Development, Active Pharmaceutical Ingredients-IV, Dr. Reddy's Laboratories Ltd., IDA Jeedimetla, Hyderabad 500055, A.P., India*
[b] *Department of Analytical Research, Discovery Research, Dr. Reddy's Laboratories Ltd., Bollaram Road, Miyapur, Hyderabad 500049, A.P., India*
[c] *Department of Chemistry, Institute of Science and Technology, J.N.T. University, Kukatpally, Hyderabad 500072, A.P., India*

Received 19 February 2007; received in revised form 23 May 2007; accepted 25 May 2007
Available online 2 June 2007

Abstract

Six impurities in pantoprazole sodium bulk drug substance were detected by a simple high performance liquid chromatographic method (HPLC) whose area percentage ranged from ~0.05 to 0.34%. Liquid chromatography–mass spectrometry (LC–MS) was performed to identify the molecular weight of the impurities. A thorough study was undertaken to characterize these impurities. These impurities were synthesized, subsequently characterized and were co-injected with the sample containing impurities and found the retention time match of the spiked impurities. Based on their spectral data (IR, NMR and MS), these impurities were characterized as; 5-(difluoromethoxy)-2-[[(3,4-dimethoxy-2-pyridinyl)methyl]thio]-1*H*-benzimidazole (Impurity-I); 5-(difluoromethoxy)-2-[[(3,4-dimethoxy-2-pyridinyl)methyl]sulfonyl]-1*H*-benzimidazole (Impurity-II); 5-(difluoromethoxy)-2-[[(3,4-dimethoxy-1-oxide-2-pyridinyl)methyl]sulfonyl]-1*H*-benzimidazole (Impurity-III); 5-(difluoromethoxy)-2-[[(3,4-dimethoxy-2-pyridinyl)methyl]thio]-1-((3,4-dimethoxy-2-pyridinyl)methyl)-1*H*-benzimidazole (Impurity-IV); 5-(difluoromethoxy)-2-[[(3,4-dimethoxy-2-pyridinyl)methyl]sulfinyl]-1-((3,4-dimethoxy-2-pyridinyl)methyl)-1*H*-benzimidazole (Impurity-V); 5-(difluoromethoxy)-2-[[(3,4-dimethoxy-1-oxide-2-pyridinyl)methyl]sulfinyl]-1*H*-benzimidazole (Impurity-VI). The formation of these impurities was proposed. The structure of the Impurity-II was unambiguously confirmed by single crystal X-ray diffraction (XRD) studies.

Keywords: Pantoprazole sodium; LC–MS; Identification; Spectroscopy; Characterization; HRMS; Single crystal and XRD studies

1. Introduction

[(Pyridylmethyl)sulfinyl] benzimidazoles (PSBs) have proved to be highly active inhibitors of the gastric (H^+, K^+)-ATPase both *in vitro* and *in vivo* with high and long lasting antisecretory activity [1,2]. Pantoprazole, 5-(difluoromethoxy)-2-[[(3,4-dimethoxy-2-pyridinyl)methyl]sulfinyl]-1*H*-benzimidazole is an oral pharmaceutically active compound having promising anti-ulcer activity [3] and belongs to the class of 2-[[(2-pyridyl)methyl]sulfinyl]-1*H*-benzimidazoles. In general these classes of compounds were used for the prevention and treatment of gastric acid related diseases [4]. Literature studies reveal different methods for the preparation of pantoprazole [5]. Some spectrophotometric methods for the determination of lansoprazole, omeprazole and pantoprazole sodium sesquihydrate were described earlier [6–10]. However, very little information was available for the determination of its impurities.

The presence of impurities in an active pharmaceutical ingredient (API) can have a significant impact on the quality and safety of the drug products. During the analysis of laboratory batches of pantoprazole sodium, six impurities with ultra violet (UV) area percentage ranging from 0.05 to 0.34% were detected, by a simple HPLC method. In order to commercialize an API, it is a mandatory requirement by regulatory authorities, to identify and characterize all the unknown impurities that

* Corresponding author. Tel.: +91 40 23045439; fax: +91 40 3045438.
E-mail address: mosesbabuj@drreddys.com (J.M. Babu).
[1] DRL Pub. No. DRL-IPDO-IPM 00034.

0731-7085/$ – see front matter © 2007 Elsevier B.V. All rights reserved.
doi:10.1016/j.jpba.2007.05.032

are present in it at a level of ≥0.10% [11]. In this context, a comprehensive study was undertaken to characterize all the six impurities present in the lab batches of pantoprazole sodium by spectroscopic and spectrometric techniques and the results are presented in this article. The pathway for the formation of these impurities was also proposed. Among the pantoprazole impurities, *N*-methylpantoprazole, Impurity-I, -II, -VI were described earlier as process related impurities [12–15], while Impurity-III and Impurity-IV are being reported for the first time here.

2. Experimental

2.1. Samples and chemicals

The investigated samples of pantoprazole sodium (Experiment No. PAN/C436/2/05) bulk material was obtained from the R&D Department, API-III, Dr. Reddy's Laboratories Ltd., Hyderabad, India. Impurities-I, -II, -III, -IV, -V and -VI were synthesized in the laboratory after identification by HPLC and determination of molecular weight by LC–MS. HPLC grade acetonitrile and acetic acid were obtained from Merck, Mumbai, India. Ammonium acetate salt, phosphoric acid and triethylamine were obtained from AR grade, SD fine chemicals Limited, Mumbai, India. Water used for preparing mobile phase was purified using Millipore Milli-Q plus (Milford, MA, USA) purification system. Chloroform-*d* and dimethylsulphoxide-d_6 were purchased from Aldrich Chemical Co., USA.

2.2. High performance liquid chromatography (HPLC)

An In-house LC gradient method was developed for the separation of all possible related substances of pantoprazole sodium. A Waters HPLC (717 plus auto sampler) equipped with 515 pump and Waters 2996-photodiode array detector (Waters Corporation, Milford, USA) was used. The buffer solution used for the preparation of mobile phases A and B consists 0.778 g of ammonium acetate (0.01 M) and 1 mL of triethyl amine in 1000 mL of water, pH adjusted (pH 4.5) with diluted phosphoric acid. Mobile phase-A was prepared in the ratio of 70:30 (v/v) of buffer and acetonitrile and Mobile phase-B was prepared in the ratio of 30:70 (v/v) of buffer and acetonitrile. Symmetry C_{18}, 250 mm × 4.6 mm, 5μ-particle size column (Waters, Ireland) was used, with a timed gradient program of *T* (min)/*%B* (v/v): 01/20, 10/20, 15/40, 20/60, 25/80, 27/20, 35/20, with a flow rate of 1.0 mL/min, column oven temperature was 30 °C and column eluent was monitored by UV at 290 nm. This LC method was able to detect all the process related substances with good resolution.

2.3. Liquid chromatography–mass spectrometry (LC–MS) and mass spectrometry

Mass spectrometry compatible chromatographic method was developed for the identification of all possible related impurities of pantoprazole sodium. The buffer solution used for the preparation of mobile phases A and B consisted of 0.778 g of ammonium acetate (0.01 M) dissolved in 1000 mL of water and pH adjusted (pH 4.5) with acetic acid. Mobile phase-A was prepared in the ratio of 70:30 (v/v) of buffer and acetonitrile and mobile phase-B was prepared in the ratio of 30:70 (v/v) of buffer and acetonitrile. Symmetry C_{18}, 250 mm × 4.6 mm, 5μ (Waters, Ireland) was used, with a timed gradient program of *T* (min)/*%B*: 01/20, 10/20, 15/40, 20/60, 25/80, 27/20, 35/20, with a flow rate of 1.0 mL/min and UV detection at 290 nm. This LC method was able to detect all the process related substances. The mass spectrum of impurities was recorded on AB-4000 Q-trap LC–MS/MS mass spectrometer.

The LC–MS Analysis was performed on AB-4000 Q-trap LC–MS/MS mass spectrometer [16]. The analysis was performed in positive ionization mode with Turbo Ion Spray interface with the following conditions: ion source voltage at 5500 V, declustering potential at 80 V, entrance potential at 10 V, with the nebuliser gas as nitrogen at 30 psi. Whereas the negative ionization was performed by switching the polarity of the ion source voltage to −4500 V.

High resolution mass spectra were analysed on the Micromass LCT Premier XE mass spectrometer equipped with an ESI Lock spray source for accurate mass values (Water Corporation, Milford, MA, USA). Leucine enkephalin was used as an internal reference compound, which was introduced via the Lock spray channel. Data were acquired using the positive and negative mode. The mass spectrometer was equipped with a Waters Aquity HPLC system. Pantoprazole sodium and its impurities were dissolved in methanol at a concentration level of 1 mg/ml, sonicated for 5 min and centrifuged for 6 min at 16,000 rpm. This was diluted 1:100 with methanol and introduced to the mass spectrometer via Infusion syringe.

2.4. NMR spectroscopy

The ^{1}H, ^{13}C and DEPT for pantoprazole sodium were done at 400 and 100 MHz on Varian Mercury plus 400 MHz FT NMR Spectrometer (Varian, Germany) and similar experiments for impurities-I, -II, -III, -IV, -V and -VI were performed on Gemini-2000 (200 MHz) in DMSO-d_6.The ^{1}H chemical shift values were reported on the δ scale in ppm, relative to TMS ($\delta = 0.00$ ppm) and the chemical shift values were reported relative to $CDCl_3$ ($\delta = 77.00$ ppm) (Cambridge Isotopic Labs, USA) and DMSO-d_6 ($\delta = 39.50$ ppm) as internal standards, respectively.

2.5. Melting point determination

Melting points of all the impurities were determined by using the capillary method on a POLMON digital melting point apparatus Model no. MP 96 (Mumbai, India).

2.6. FT-IR spectroscopy

The IR spectra were recorded in the solid state as KBr dispersion medium using FT-IR (Perkin Elmer, Spectrum One) spectrophotometer.

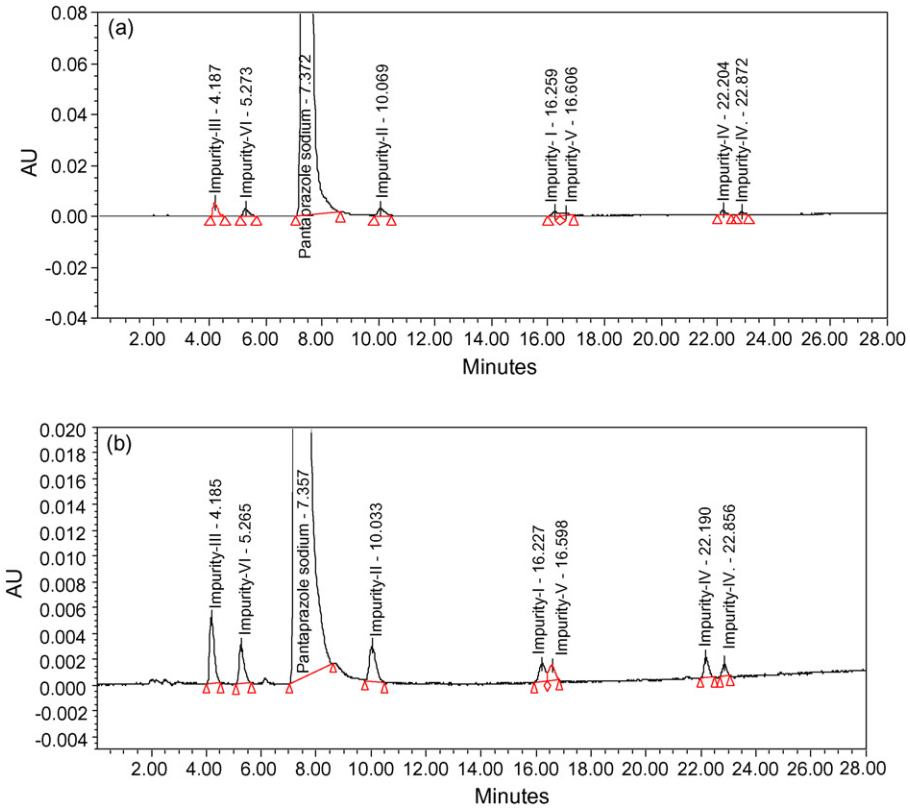

Fig. 1. (a) HPLC chromatogram of pantoprazole sodium laboratory sample. (b) HPLC chromatogram of pantoprazole sodium laboratory sample spiked with six impurities.

2.7. Single crystal XRD studies

Single crystals suitable for X-ray diffraction were grown from chloroform and benzene. The intensity data was collected on Rigaku AFC-7S single crystal diffractometer [17] using Mo Kα radiation (λ = 0.7107 Å) with CCD Mercury area detector. The structure was solved by direct methods SIR92 [18] and refined using least squares procedures with the Crystal Structure software [19].

2.8. Synthesis of impurities

The Impurity-I is one of the key intermediate in the preparation of pantoprazole; Impurity-II was synthesized by further oxidation of pantoprazole using *m*-chloroperbenzoic acid (*m*-CPBA) as an oxidizing agent. Impurity-III was synthesized by further oxidation of Impurity-II using *m*-CPBA, Impurity-IV was synthesized by the condensation of Impurity-I and pantoprazole chloro compound (a key starting material, 2-chloromethyl-3,4-dimethoxy pyridine hydrochloride) in the presence of sodium hydroxide as a base; Impurity-V was synthesized by further oxidation of Impurity-IV using *m*-CPBA as an oxidizing agent; Impurity-V preparation is a three-step process, synthesis consist of N-oxide preparation from its chloro compound using *m*-CPBA, followed by condensation with 5-difluoromethoxy-2-mercapto-1*H*-benzimidazole and then oxidation of obtained sulfide compound using *m*-CPBA.

3. Results and discussion

3.1. Detection of impurities-I, -II, -III, -IV, -V and -VI

A typical analytical LC chromatogram of a laboratory batch of pantoprazole sodium bulk drug recorded using the LC method is described in Section 2.2. The LC–MS compatible method which is used to detect the impurities is described in Section 2.3 (Fig. 1). Retention times in HPLC and structures of these impurities and pantoprazole sodium are shown in Table 1. Impurities-VI and -III are polar and Impurity-II, -I, -V (one isomer) and Impurity-IV (both positional isomers) are non-polar, respectively with respect to pantoprazole sodium.

3.2. Structural elucidation of pantoprazole and its impurities

The +ve electrospray ionization (ESI) spectrum of the impurity showed peaks at *m/z* 367.9, 735.7, 389.9 and 757.1 corresponding to the adduct ions $(M+H)^+$, $(2M+H)^+$, $(M+Na)^+$ and $(2M+Na)^+$. The −ve ES-MS spectrum showed deprotonated molecular ion peak at *m/z* 365.9 $(M-H)^-$.

The DEPT spectra displayed one negative signal due to one methylene group and eight positive peaks due to the presence of two methyl groups and the rest are due to the methine groups. IR spectrum displayed characteristic absorptions at 1588, 1305 and 1124 cm^{-1} corresponding to C=C, C–N and C–F stretching which was supported by the appearance of the

Table 1
HPLC retention time, molecular weight (MW) from LC–MS, nature of the compounds and atom numbering used for NMR assignment of the impurities

S. no.	Retention time[a] (min)	Compound	MW	Structure	Nature
1	16.26	Impurity-I	367	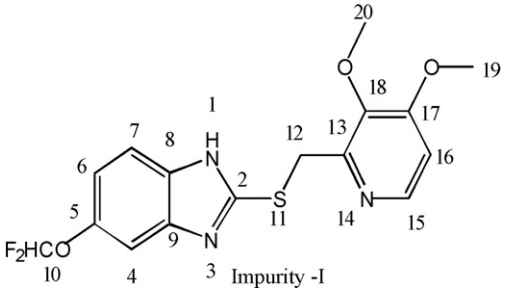 Impurity -I	Process related
2	10.06	Impurity-II	399	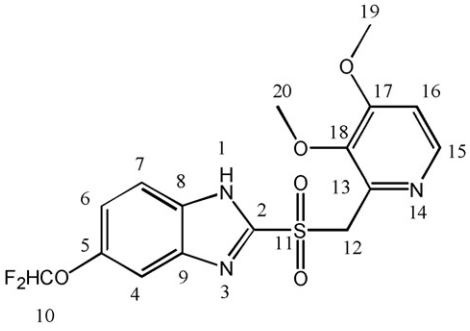 Impurity -II	Process related
3	5.27	Impurity-III	415	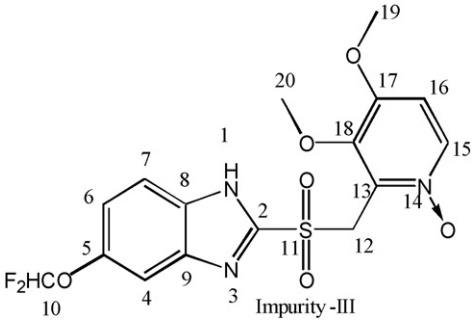 Impurity -III	Process related
4	7.37	Pantoprazole sodium	383	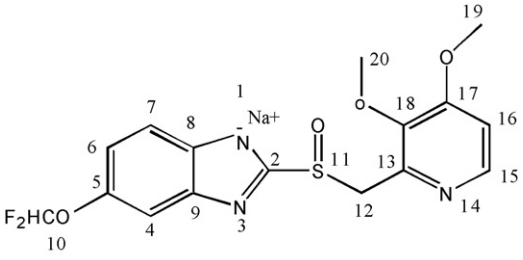 Pantoprazole sodium	API
5	22.20, 22.87	Impurity-IV[b]	518	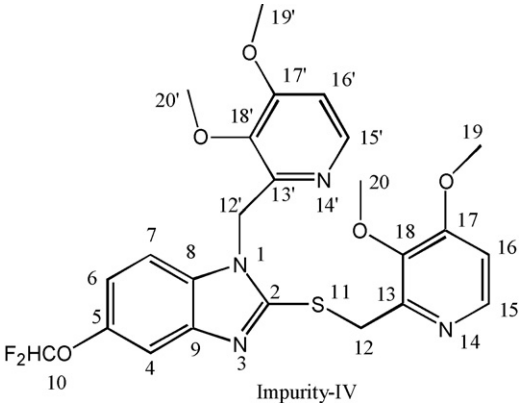 Impurity-IV	Process related

Table 1 (*Continued*)

S. no.	Retention time[a] (min)	Compound	MW	Structure	Nature
6	16.60	Impurity-V	534	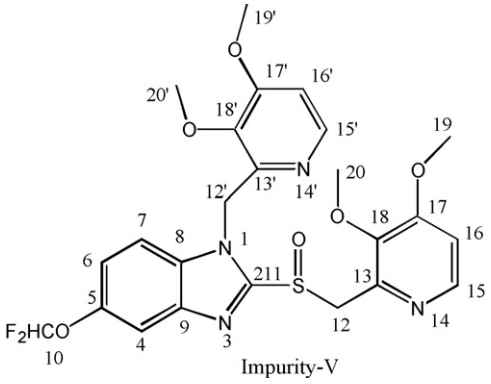 Impurity-V	Process related
7	4.18	Impurity-VI	399	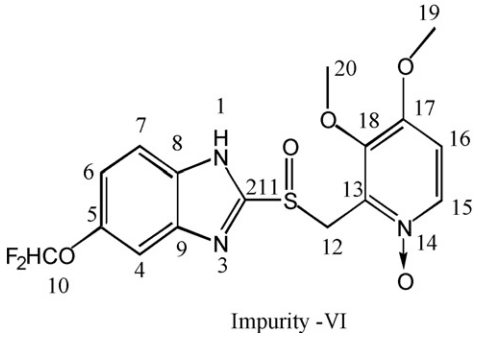 Impurity -VI	Process related

[a] Retention time of compounds in HPLC.
[b] This impurity contains two positional isomers.

quaternary carbon signal characteristic of a C=N group in ^{13}C NMR spectrum. The peaks at 1281, 1172 and 1038 cm^{-1} in the IR spectrum are indicative of ether functionality. Based on the above spectral data the molecular formula of Impurity-I could be $C_{16}H_{15}F_2N_3O_3S$. This molecular formula matched well with the protonated molecular ion observed at *m/z* 367.9 in the mass spectral data. The data obtained from the spectral studies can be rationalized in terms of Impurity-I having the molecular formula $C_{16}H_{15}F_2N_3O_3S$ and the corresponding structure was characterized as 5-(difluoromethoxy)-2-[[(3,4-dimethoxy-2-pyridinyl)methyl]thio]-1*H*-benzimidazole (retention time = 16.26).

The spectral data of pantoprazole is compared with those of impurities-I to -VI. It is interesting to note that Impurity-I, -II, -III and -VI have the same skeletal system as evident by the number of NMR signals. The mass spectra of the Impurity-I and -II displayed protonated molecular ion at *m/z* 367.9 and 400.4, which is 16 amu less and 16 amu more than that of pantoprazole (molecular ion *m/z* 383), respectively. The chemical shift of methylene carbon adjacent to sulphur appeared at 32.82 and 57.38 ppm for Impurity-I and Impurity-II, respectively. Thus the Impurity-I and Impurity-II structure can be explained in terms of removal and addition of oxygen on sulphur, respectively from pantoprazole.

Though the protonated molecular ion for both Impurity-II (*m/z* 400.4) (retention time = 10.06) and Impurity-VI (*m/z* 400.3) (retention time = 4.18) was same, the diagnostic change in the aromatic protons in pyridine moiety in Impurity-VI indicates the formation of N-oxide impurity of pantoprazole. Similarly on comparison of Impurity-II with Impurity-III (retention time = 5.27), the chemical shift change in the aromatic protons in the pyridine moiety indicates that Impurity-III is an N-oxide of Impurity-II.

The spectral data of Impurity-IV (retention time = 22.20, 22.87) have several additional resonances both in the aliphatic and aromatic region. The protonated molecular ion at *m/z*, 519.0 can be attributed to the *N*-alkylated product of Impurity-I and 2-chloromethyl-3,4-dimethoxy pyridine hydrochloride moiety.

The mass spectra of the Impurity-V (retention time = 16.60) displayed protonated molecular ion at *m/z* 535.3, which is 16 amu more than that of Impurity-IV (protonated molecular ion *m/z* 519.0). The chemical shift of methylene carbon adjacent to sulphur appeared at 34.96 and 56.59 ppm for Impurity-IV and Impurity-V, respectively. Thus the Impurity-V structure can be explained in terms of the addition of oxygen on sulphur in Impurity-IV. The spectral data used for elucidation of the Impurities from I to VI, are tabulated (Figs. 1 and 2 and Tables 1–3).

3.2.1. Single crystal XRD studies of Impurity-II

The molecular structure of Impurity-II is further confirmed by single crystal XRD studies. Impurity-II crystallizes in the monoclinic space group $P2_1/n$ from methanol with cell dimensions $a = 11.51(1)$ Å, $b = 7.896(9)$ Å, $c = 19.27(2)$ Å, $\beta = 97.45(2)^\circ$, $V = 1737(3)$ Å^3 containing four molecules in the unit cell. The structure was solved by direct methods with the final *R* value of 0.092 with 4286 unique reflections. All

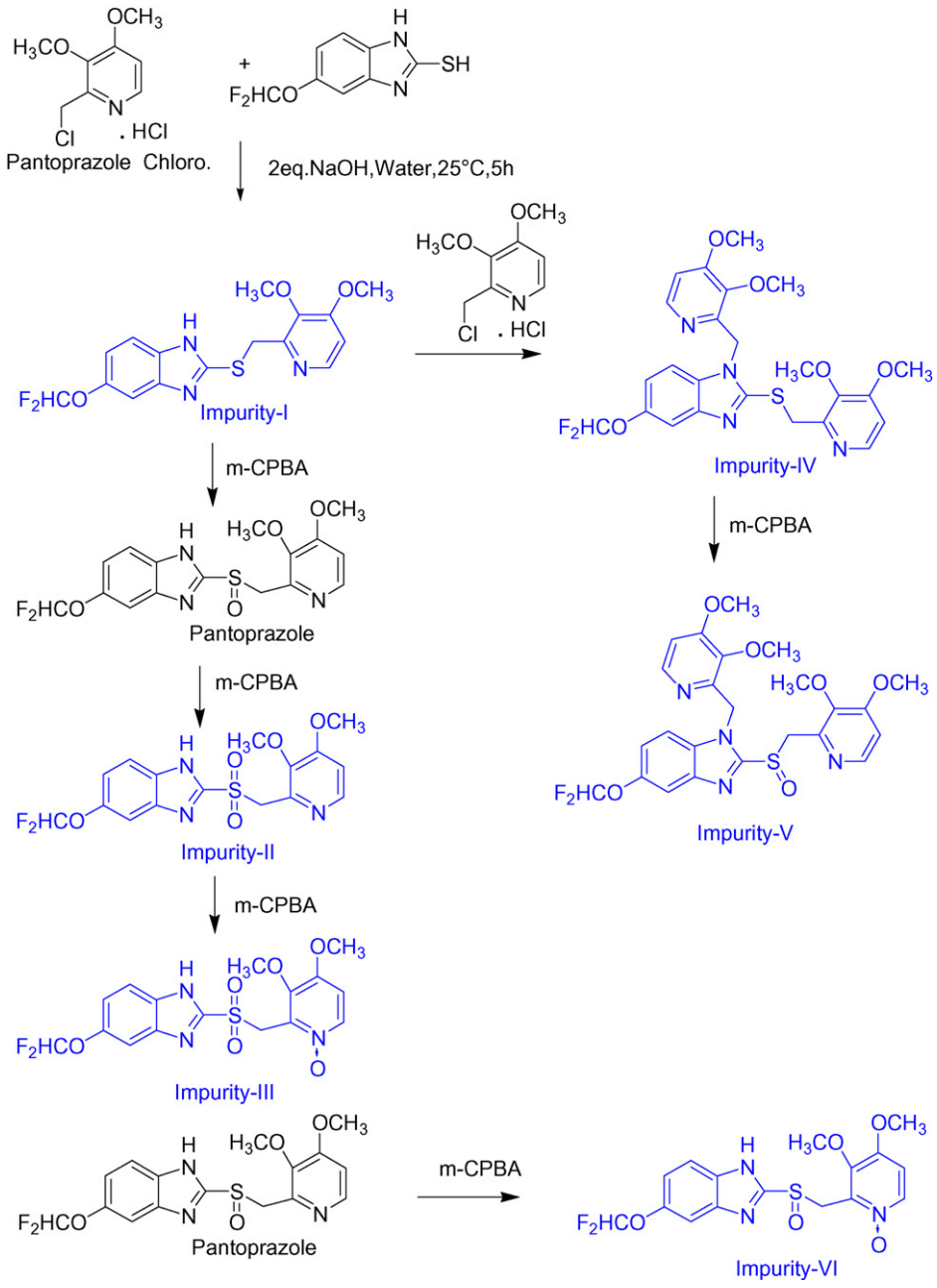

Fig. 2. Formation of impurities.

the H's were included in the refinement at calculated positions, in the riding model approximation with C–H bond distances of 0.950 Å. An absorption correction was applied using the multi-scan method. Thus, the structure of Impurity-II is determined as 5-(difluoromethoxy)-2-[[(3,4-dimethoxy-2-pyridinyl)methyl]sulfonyl]-1*H*-benzimidazole.

All the bond parameters are found to be normal [20]. The angle between the benzimidazole and the pyridinyl ring is 14.282(3)°. The methylsulfonyl group, which adopts trans conformation, links the benzimidazole and pyridinyl, rings. The molecules are held together in the lattice by intermolecular and intramolecular hydrogen bonds, the hydrogen bonding geometry is given in Fig. 3.

3.3. Formation of impurities

One of the intermediate used in the synthesis of pantoprazole was Impurity-I. Pantoprazole on further oxidation yields Impurity-II, -VI and then Impurity-III. Due to the condensation of pantoprazole chloro compound with Impurity-I, 5-(difluoromethoxy)-2-[[(3,4-dimethoxy-2-pyridinyl)methyl]thio]-1-((3,4-dimethoxy-2-pyridinyl)methyl)-1*H*-benzimidazole (Impurity-IV, two positional isomers, 5-difluoromethoxy analogue and 6-difluoromethoxy analogue) are formed which undergo oxidation to Impurity-V. The schematic diagram for the formation of Impurities-I, -II, -III, -IV, -V and -VI are shown in Fig. 2.

Table 2
Melting range, FT-IR, mass spectral data of pantoprazole sodium and its impurities-I, -II, -III, -IV, -V and -VI

S. no.	Compound	Melting point (°C)	IR[a] (cm^{-1})	MS analysis
1.	Impurity-I	165–170	3546 (N–H stretching), 3256 (aromatic C–H stretching), 2942, 2877 (aliphatic C–H stretching), 1588, 1485 (aromatic C=C stretching), 1379, 1366 (aliphatic C–H bending), 1305 (C–N stretching), 1281, 1172, 1124 (C–F stretching), 1038 (C–O stretching), 860, 805 (aromatic C–H bending)	+ve ES-MS: 367.9 $(M+H)^+$, 735.7 $(2M+H)^+$, 389.9 $(M+Na)^+$, 757.1 $(2M+Na)^+$. HRMS: *m/z* calcd for $(M+H)^+$ $C_{16}H_{16}N_3O_3F_2S$: 368.0880; found: 368.0883 (ppm: 0.8). −ve ES-MS:365.9 $(M-H)^-$. HRMS: *m/z* calcd for $(M-H)^-$. $C_{16}H_{14}N_3O_3F_2S$: 366.0724; found: 366.0723 (ppm: −0.3)
2.	Impurity-II	145–150	3111 (aromatic C–H stretching), 2946, 2842 (aliphatic C–H stretching), 1588, 1499, 1453, 1427 (aromatic C=C, stretching), 1383 (aliphatic C–H bending), 1305 (C=N stretching), 1282, 1187, 1044 (C–O stretching), 1131 (C–F stretching) 1067 (S=O stretching), 824 (aromatic C–H bending)	+ve ES-MS: 400.4 $(M+H)^+$, 422.0 $(M+Na)^+$, 821.2 $(2M+Na)^+$, 416.0 $(M+NH_3)^+$. HRMS: *m/z* calcd for $(M+H)^+$ $C_{16}H_{16}N_3O_5F_2S$: 400.0779; found: 400.0792 (ppm: 3.2). −ve ES-MS: 397.8 $(M-H)^-$. HRMS: *m/z* calcd for $(M-H)^-$. $C_{16}H_{14}N_3O_5F_2S$: 398.0622; found: 398.0623 (ppm: 0.3)
3.	Impurity-III	158–162	3412 (moisture O–H stretching), 3104 (aromatic C–H stretching), 2973, 2900 (aliphatic C–H stretching), 1495, 1471, 1435 (aromatic C=C stretching), 1336 (aliphatic C–H bending), 1307 (C=N stretching), 1288, 1085 (C–O stretching), 1131 (C–F stretching), 1052, 1040 (S=O stretching), 757 (aromatic C–H bending)	+ve ES-MS: 415.8 $(M+H)^+$, 437.9 $(M+Na)^+$, 852.9 $(2M+Na)^+$. HRMS: *m/z* calcd for $(M+H)^+$ $C_{16}H_{16}N_3O_6F_2S$: 416.0728; found: 416.0725 (ppm: −0.7). −ve ES-MS: 413.8 $(M-H)^-$. HRMS: *m/z* calcd for $(M-H)^-$. $C_{16}H_{14}N_3O_6F_2S$: 414.0571; found: 414.0579 (ppm: 1.9)
4.	Impurity-IV	135–138	3451 (moisture O–H stretching), 2982 (aromatic C–H stretching), 2944, 2839 (aliphatic C–H stretching), 1588, 1489, 1445, 1434 (aromatic C=C stretching), 1372, 1350 (aliphatic C–H bending), 1300 (C=N stretching), 1229, 1173, 1065 (C–O stretching), 1120 (C–F stretching), 826, 815 (aromatic C–H bending).	+ve ES-MS: 519.0 $(M+H)^+$, 541.0 $(M+Na)^+$, 557.0 $(M+K)^-$. HRMS: *m/z* calcd for $(M+H)^+$ $C_{24}H_{25}N_4O_5F_2S$: 519.1514; found: 519.1506 (ppm: −1.5). −ve ES-MS: 517.0 $(M-H)^-$. HRMS: *m/z* calcd for $(M+Cl)^-$ $C_{24}H_{24}N_4O_5F_2SCl$: 553.1124; found: 553.1123 (ppm: −0.2)
5.	Impurity-V	145–149	3423 (moisture O–H stretching), 3038 (aromatic C–H stretching), 2979, 2944 (aliphatic C–H stretching), 1586, 1489, 1446, 1421 (aromatic C=C stretching), 1371, 1352 (aliphatic C–H bending), 1300 (C=N stretching), 1262, 1173, 1111 (C–F stretching), 1061 (S=O stretching), 1047 (C–O stretching), 816 (aromatic C–H bending)	+ve ES-MS: 535.3 $(M+H)^+$, 1069.6 $(2M+H)^+$, 557.1 $(M+Na)^+$, 1091.6 $(2M+Na)^+$. HRMS: *m/z* calcd for $(M+H)^+$ $C_{24}H_{25}N_4O_6F_2S$: 535.1463; found: 535.1461 (ppm: −0.4). HRMS: *m/z* calcd for $(M+Cl)^-$ $C_{24}H_{24}N_4O_6F_2SCl$: 569.1073; found: 569.1088 (ppm: 2.6)
6.	Impurity-VI	165–170	3468 (moisture O–H stretching), 3112 (aromatic C–H stretching), 2946, 2841 (aliphatic C–H stretching), 1496, 1472, 1432, 1389 (aromatic C=C stretching), 1389, 1358 (aliphatic C–H bending), 1309 (C=N stretching), 1275, 1166, 1023 (C–O stretching), 1121 (C–F stretching), 1063 (S=O stretching), 831 (aromatic C–H bending)	+ve ES-MS: 400.3 $(M+H)^+$, 422.3 $(M+Na)^+$, 821.1 $(2M+Na)^+$, 438.5 $(M+K)^+$. HRMS: *m/z* calcd for $(M+H)^+$ $C_{16}H_{16}N_3O_5F_2S$: 400.0779; found: 400.0786 (ppm: 1.7). −ve ES-MS: 399.9 $(M-H)^-$. HRMS: *m/z* calcd for $(M-H)^-$ $C_{16}H_{14}N_3O_5F_2S$: 398.0622; found: 398.0622 (ppm: 0.0)
7.	Pantoprazole sodium	141–161 (dec.)[b]	3488 (moisture O–H stretching), 3181 (aromatic C–H stretching), 2998, 2942 (aliphatic C–H stretching), 1590, 1491, 1465, 1450, 1428 (aromatic C=C stretching), 1363, 1376 (aliphatic C–H bending), 1305 (C=N stretching), 1277, 1171, 1042 (C–O stretching), 1121 (C–F stretching), 1073 (S=O stretching), 837 (aromatic C–H bending)	+ve ES-MS: 383.9 $(M+H)^+$, 1151.0 $(3M+H)^+$, 406.4 $(M+Na)^+$, 789.9 $(2M+Na)^+$. HRMS: *m/z* calcd for $(M+H)^+$ $C_{16}H_{16}N_3O_4F_2S$: 384.0830; found: 384.0832 (ppm: 0.5). −ve ES-MS: 381.8 $(M-H)^-$. HRMS: *m/z* calcd for $(M-H)^-$ $C_{16}H_{14}N_3O_4$ F_2S: 382.0673; found: 382.0672 (ppm: −0.3)

[a] KBr (Impurities-I, -II, -III, -IV, -V, -VI and pantoprazole sodium).
[b] Melting with decomposition.

Table 3
^{1}H and ^{13}C NMR assignments for pantoprazole sodium and impurities-I, -II, -III, -IV, -V and -VI

Position[a]	Pantoprazole sodium				Impurity-I				Impurity-II				Impurity-III			
	^{1}H	ppm/J	^{13}C	DEPT	^{1}H	ppm/J	^{13}C	DEPT	^{1}H	ppm/J	^{13}C	DEPT	^{1}H	ppm/J	^{13}C	DEPT
1	–	–	–	–	NH	12.76/br	–	–	NH	13.9/br	–	–	NH	13.9/br	–	–
2	–	–	164.10	–	–	–	151.86	–	–	–	149.52	–	–	–	134.92	–
4	1H	7.2/d, 2.2	107.50	CH	1H	7.28/br	104.94	CH	1H	7.47/br	106.37	CH	1H	7.45/br	106.36	CH
5	–	–	146.89	–	–	–	149.55	–	–	–	147.99	–	–	–	147.93	–
6	1H	6.8/dd (8.6, 2.3)	112.45	CH	1H	6.97 dd (2.4, 8.4)	113.58	CH	1H	7.23/dd (2.4, 9.2)	117.34	CH	1H	7.23/dd (2.0, 8.0)	117.20	CH
7	1H	7.4/d, 8.6	117.53	CH	1H	7.47/d (8.4)	113.75	CH	1H	7.75/d (9.2)	118.50	CH	1H	7.73/d (8.0)	118.46	CH
8	–	–	144.60	–	–	–	142.95	–	–	–	138.42	–	–	–	138.36	–
9	–	–	145.88	–	–	–	140.00	–	–	–	136.19	–	–	–	136.16	–
10	1H	7.0/t, 76	117.53	CH	1H	7.16/t (74.8)	116.96 t (255.9)[b]	CH	1H	7.28/t (74.4)	116.71/t (256.7)[b]	CH	1H	7.27/t (74.4)	117.20 t (256.6)[b]	CH
12	Ha	4.7/d, 13.0	57.16	CH_2	2H	4.67/s	32.82	CH_2	2H	4.98/s	57.38	CH_2	2H	5.23/s	52.61	CH_2
	Hb	4.3/d, 13.0	–	–	–	–	–		–	–	–	–	–	–		–
13	–	–	144.60	–	–	–	149.55	–	–	–	141.63	–	–	–	146.07	–
15	1H	8.2/d, 5.5	146.65	CH	–	8.16/d (5.6)	145.97	CH	1H	7.98/d (5.2)	145.64	CH	1H	8.02/d (7.2)	134.51	CH
16	1H	7.1/d, 5.5	107.98	CH	–	7.09/d (5.6)	108.19	CH	1H	7.09/d (5.2)	108.97	CH	1H	7.19/d (7.2)	109.97	CH
17	–	–	158.36	–	–	–	158.21	–	–	–	158.37	–	–	–	150.39	–
18	–	–	158.36	–	–	–	145.48	–	–	–	144.98	–	–	–	150.46	–
19	3H	3.8/s	55.94	CH_3	3H	3.90/s	55.93	CH_3	3H	3.89/s	55.99	CH_3	3H	3.91/s	56.61	CH_3
20	3H	3.9/s	60.95	CH_3	3H	3.81/s	60.57	CH_3	3H	3.77/s	60.69	CH_3	3H	3.80/s	61.15	CH_3

Table 3 (*Continued*)

Position[a]	Impurity-IV				Impurity-V				Impurity-VI			
	^{1}H	ppm/J	^{13}C	DEPT	^{1}H	ppm/J	^{13}C	DEPT	^{1}H	ppm/J	^{13}C	DEPT
1	–	–	–	–	–	–	–	–	NH	13.8/br	–	–
2	–	–	149.14	–	–	–	155.07	–	–	–	156.30	–
4	1H	7.30/d (2.0)	101.50	CH	1H	7.47/d (2.0)	102.06	CH	1H	7.37/br	103.50	CH
5	–	–	147.75	–	–	–	147.87	–	–	–	br[c]	–
6	1H	6.98/m	110.54	CH	1H	7.16/dd (2.0, 8.8)	115.46	CH	1H	7.69/br	122.00	CH
7	1H	7.59/d (8.8)	118.18	CH	1H	7.84/d (8.8)	121.28	CH	1H	7.20/br	116.10	CH
8	–	–	134.43	–	–	–	136.31	–	–	–	br[c]	–
9	–	–	137.09	–	–	–	139.08	–	–	–	br[c]	–
10	1H	7.15/t (74.8)	116.95 t (255.7)	CH	1H	7.20/t (74.0)	116.61 t (255.9)	CH	1H	7.24/t (74.4)	116.81 t (255.9)[b]	CH
12, 12′	2H 2H	4.66/s 5.44/s	34.96 44.26	CH_2	Ha Hb 2H	4.62/d (13.6) 5.01/d (13.2) 5.81q (16.8)	56.59 44.23	CH_2	2H	4.80/dd (12.0, 14.8)	52.01	CH_2
13, 13′	–	–	–	–	–	–	142.30	–	–	–	136.63	–
15, 15′	1H 1H	8.13/d (5.2) 8.04/d (5.6)	147.78 145.44	CH	1H 1H	8.17/d (5.2) 8.03/d (5.6)	147.60 145.86	CH	1H	8.19/d (7.2)	134.71	CH
16, 16′	1H 1H	7.08/d (5.6) 7.07/d (5.6)	108.37 108.15	CH	1H 1H	7.09/d (5.2) 7.07/d (5.6)	108.47 108.32	CH	1H	7.21/d (7.2)	109.54	CH
17, 17′	–	–	153.17, 153.89	–	–	–	145.45	–	–	–	150.62	–
18, 18′	–	–	158.07, 158.03	–	–	–	158.35, 158.12	–	–	–	146.27	–
19, 19′	3H 3H	3.78/s 3.77/s	60.48 60.38	CH_3	6H	3.89/s	55.97 55.92	CH_3	3H	3.90/s	56.55	CH_3
20, 20′	3H 3H	3.89/s 3.87/s	55.89	CH_3	3H 3H	3.87/s 3.72/s	60.76 60.42	CH_3	3H	3.71/s	61.43	CH_3

s, singlet; d, doublet; dd, doublet of doublet; t, triplet; m, multiplet; dt, doublet of triplet; br, broad. 12′–20′ applicable for Impurity-IV and -V.

[a] Refer the structural formula (Table 1) for numbering.

[b] Splitting due to coupling between ^{19}F and ^{13}C.

[c] Signals not observed.

(a)

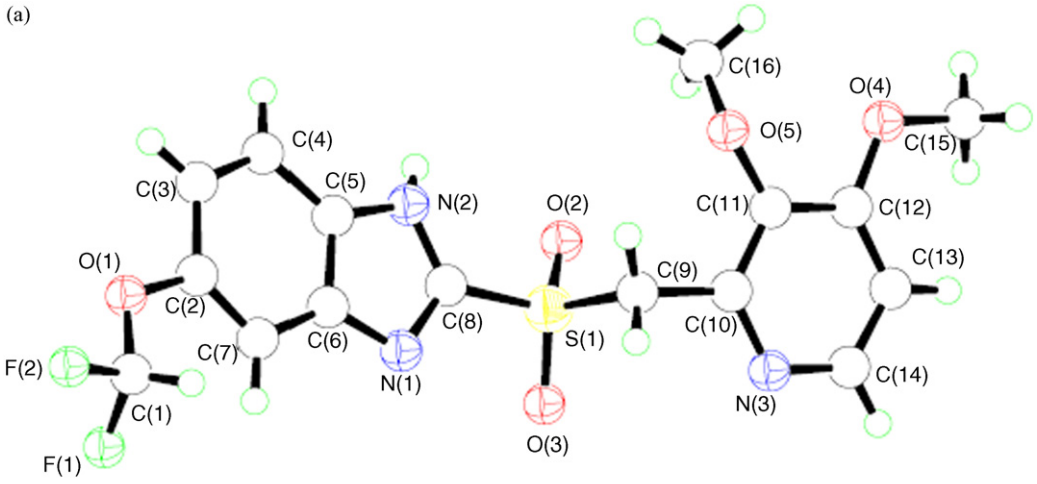

(b)

D-H...A	D - H	H...A	D...A	D - H...A	symmetry
C7-H1... F1	0.9500	2.5100	3.033(12)	115.00	x, y, z
C7-H1...O3	0.9500	2.5800	3.117(12)	116.00	1/2-x,-1/2+y, 1/2-z
C15-H6...O2	0.9500	2.5500	3.337(16)	140.00	x, 1+y,z
C16-H9...O4	0.9500	2.5300	2.883(19)	102.00	x, y, z
C9-H12…O5	0.9500	2.3200	2.741(13)	106.00	x, y, z

Fig. 3. (a) Molecular structure of Impurity-II and (b) hydrogen bonding geometry of Impurity-II.

4. Conclusion

The process related impurities in pantoprazole sodium bulk drug were identified, synthesized and characterized using HPLC, LC–MS, IR and NMR (^{1}H, ^{13}C and DEPT) techniques. Impurity-II was confirmed unambiguously by single crystal XRD studies.

Acknowledgements

The authors wish to thank the management of Dr. Reddy's Laboratories Limited, Dr. Apurba Bhattacharya (Vice President, IPDO-R&D), colleagues of Analytical Research Department of Discovery Research and the colleagues of API-III, Dr. Reddy's Laboratories Ltd. for their constant encouragement and excellent cooperation.

References

[1] B. Wallmark, P. Lorentzon, H. Larsson, J. Gastroenterol. 20 (1985) 37–51.
[2] H. Larsson, E. Carlsson, U. Junggren, l. Olbe, S.E. Sjostrand, I. Skanberg, G. Sundell, Gastroenterology 85 (1983) 900–907.
[3] B. Kohl, E. Sturm, J. Senn-Bilfinger, W.A. Simon, U. Kruger, H. Schaefer, G. Rainer, V. Figala, K. Klemm, J. Med. Chem. 35 (1992) 1049–1057.
[4] B. Kohl, E. Sturm, G. Rainer, US 4,758,579, EP 166287.
[5] (a) W. Kormer, B. Kohl, Drugs of the future 15 (1990) 801–804;
(b) M. Bekhazi, M. Zoghbi, WO 97/29103.;
(c) Brennan, J. Patrick, Turner, A. Timothy, WO 99/47514 A1.
[6] A.A.M. Moustafa, J. Pharm. Biomed. Anal. 22 (2000) 45–58.
[7] O. Peres, C.H. Oliveira, R.E. Barrientos-Astigarraga, V.M. Rezende, G.P. Mendes, G. De Nucci, Arzneim. Forsch./Drug Res. 54 (2004) 314–319.
[8] A. Ekpe, T. Jacobsen, Drug Dev. Ind. Pharm. 25 (1999) 1057–1065.
[9] A.M. Mansour, O.M. Sorour, Chromatographia 53 (2001) S478–S479.
[10] Z.A. El-Sherif, A.O. Mohamed, M.G. El-Bardicy, M.F. El-Tarras, Chem. Pharm. Bull. 54 (2006) 814–818.
[11] ICH harmonized tripartite guideline, Impurities in new drug substances Q3A (R), February 2002.
[12] A.B. Adnan, N.N. Lina, M.M. Al Omari, H.D. Nidal, K.A. Mahmoud, M.A. Ahmad, A.M.Y. Jaber, Anal. Profiles Drug Subst. Excipients, 29, Academic Press, An Elsevier Science Imprint, 2002, pp. 213–259.
[13] V.T. Mathad, S. Govindan, N.K. Kolla, M. Maddipatla, E. Sajja, V. Sundaram, Org. Process Res. Dev. 8 (2004) 266–270.
[14] D. Agbaba, D. Novovic, K. Karljikovic-Rajic, V. Marinkovic, J. Planar-Chromatogr.: Mod. TLC 17 (2004) 169–172.
[15] K. Karljikovic-Rajic, D. Novovic, V. Marinkovic, D. Agbaba, J. Pharm. Biomed. Anal. 32 (2003) 1019–1027.
[16] LC/MS/MS analysis instrument Make; MDS SCIEX, Vendor name; Applied Biosystems Address: 850, Lincon Center Drive, Foster City, California, USA.
[17] J.W. Pflugrath Rigaku Corporation, Crystal Clear Software, User's Guide, Molecular Structure Corporation© 2000, 1999;
J.W. Pflugrath Rigaku Corporation, Acta Crystallogr. D 55 (1999) 1718–1725.
[18] A. Altomare, M. Cascarano, C. Glacovazzo, A. Guagliardi, J. Appl. Crystallogr. 26 (1993) 343–350.
[19] Single Crystal Structure Analysis Softaware, Rigaku/MSC, The Woodlands, TX, USA, Rigaku, Akishima, Tokyo, Japan.
[20] F.H. Allen, O. Kennard, D.G. Watson, L. Brammer, A.G. Orpen, R.J. Taylor, Chem. Soc., Perkin Trans. 2 (1987) S1–S19.